

Metadata of the chapter that will be visualized online

Chapter Title	Exponential Rosenbrock Methods and Their Application in Visual Computing	
Copyright Year	2021	
Copyright Holder	The Author(s), under exclusive license to Springer Nature Switzerland AG	
Corresponding Author	Family Name Particle Given Name Suffix Division	Luan Vu Thai Department of Mathematics and Statistics
	Organization Address Email	Mississippi State University Starkville, MS, USA luan@math.msstate.edu
Author	Family Name Particle Given Name Suffix Division	Michels Dominik L. Computational Sciences Group, Visual Computing Center
	Organization Address Email	King Abdullah University of Science and Technology Thuwal, Saudi Arabia dominik.michels@kaust.edu.sa
Abstract	We introduce a class of explicit exponential Rosenbrock methods for the time integration of large systems of stiff differential equations. Their application with respect to simulation tasks in the field of visual computing is discussed where these time integrators have shown to be very competitive compared to standard techniques. In particular, we address the simulation of elastic and nonelastic deformations as well as collision scenarios focusing on relevant aspects like stability and energy conservation, large stiffnesses, high fidelity and visual accuracy.	
Keywords (separated by “-”)	Accurate and efficient simulation - (Explicit) exponential Rosenbrock integrators - Stiff order conditions - Stiff elastodynamic problems - Visual computing	

Exponential Rosenbrock Methods and Their Application in Visual Computing

1
2
3

Vu Thai Luan and Dominik L. Michels

4

1 Introduction

5

Developing numerical models for practical simulations in science and engineering 6 usually results in problems regarding the presence of wide-range time scales. These 7 problems involve both slow and fast components leading to rapid variations in the 8 solution. This gives rise to the so-called *stiffness phenomena*. Typical examples 9 are models in molecular dynamics (see e.g. [36]), chemical kinetics, combustion, 10 mechanical vibrations (mass-spring-damper models), visual computing (specially 11 in computer animation), computational fluid dynamics, meteorology, etc., just to 12 name a few. They are usually formulated as systems of stiff differential equations 13 which can be cast in the general form 14

$$u'(t) = F(u(t)), \quad u(t_0) = u_0, \quad (1)$$

where $u \in \mathbb{R}^n$ is the state vector and $F : \mathbb{R}^n \longrightarrow \mathbb{R}^n$ represents the vector field. The 15 challenges in solving this system are due to its stiffness by means of the eigenvalues 16 of the Jacobian matrix of F differing by several orders of magnitude. In the early 17 days of developing numerical methods for ordinary differential equations (ODEs), 18 classical methods such as the explicit Runge–Kutta integrators were proposed. For 19 stiff problems, however, they are usually limited by stability issues due to the CFL 20 condition leading to the use of unreasonable time steps, particularly for large-scale 21

V. T. Luan (✉)

Department of Mathematics and Statistics, Mississippi State University, Starkville, MS, USA
e-mail: luan@math.msstate.edu

D. L. Michels

Computational Sciences Group, Visual Computing Center, King Abdullah University of Science
and Technology, Thuwal, Saudi Arabia
e-mail: dominik.michels@kaust.edu.sa

applications. The introduction of implicit methods such as semi-implicit, IMEX (see [2]), and BDF methods (see [10, 14]) has changed the situation. These standard methods require the solution of nonlinear systems of equations in each step. As the stiffness of the problem increases, considerably computational effort is observed. This can be seen as a shortcoming of the implicit schemes.

In the last 20 years, with the new developments of numerical linear algebra algorithms in computing matrix functions [1, 25, 41], exponential integrators have become an alternative approach for stiff problems (see the survey [24]; next to physics simulations, exponential integrators are nowadays also employed for different applications as for the construction of hybrid Monte Carlo algorithms, see [7]). For the fully nonlinear stiff system (1), we mention good candidates, the so-called *explicit exponential Rosenbrock methods*, which can handle the stiffness of the system in an explicit and very accurate way. This class of exponential integrators was originally proposed in [23] and further developed in [26, 30, 32, 34]. They have shown to be very efficient both in terms of accuracy and computational savings. In particular, the lower-order schemes were recently successfully applied to a number of different applications [8, 15, 17, 46, 49] and very recently the fourth- and fifth-order schemes were shown to be the method of choice for some meteorological models (see [35]).

In this work, we show how the exponential Rosenbrock methods (particularly higher-order schemes) can be also applied efficiently in order to solve problems in computational modeling of elastodynamic systems of coupled oscillators (particle systems) which are often used in visual computing (e.g. for computer animation). In their simplest formulation, their dynamics can be described using Newton's second law of motion leading to a system of second-order ODEs of the form

$$m_i \ddot{x}_i + \sum_{j \in \mathcal{N}(i)} k_{ij} (\|x_i - x_j\| - \ell_{ij}) \frac{x_i - x_j}{\|x_i - x_j\|} = g_i(x_i, \dot{x}_i, \cdot), \quad i = 1, 2, \dots, N, \quad (2)$$

where N is the number of particles, $x_i \in \mathbb{R}^3$, m_i , k_{ij} , ℓ_{ij} denote the position of particle i from the initial position, its mass, the spring stiffness, the equilibrium length of the spring between particles i and j , respectively, and $\mathcal{N}(i)$ denotes the set of indices of particles that are connected to particle i with a spring (the neighborhood of particle i). Finally, g_i represents the external force acting on particle i which can result from an external potential, collisions, etc., and can be dependent of all particle positions, velocities, or external forces set by user interaction.

Our approach for integrating (2) is first to reformulate it in the form of (1) (following a novel approach in [40]). The reformulated system is a very stiff one since the linear spring forces usually possess very high frequencies. Due to the special structure of its linear part (skew-symmetric matrix) and large nonlinearities, we then make use of exponential Rosenbrock methods. Moreover, we propose to use the improved algorithm in [35] for the evaluation of a linear combination

of φ -functions acting on certain vectors v_0, \dots, v_p , i.e. $\sum_{k=0}^p \varphi_k(A)v_k$ which is crucial for implementing exponential schemes. Our numerical results on a number of complex models in visual computing indicate that this approach significantly reduces computational time over the current state-of-the-art techniques while maintaining sufficient levels of accuracy.

This chapter is organized as follows. In Sect. 2, we present a reformulation of systems of coupled oscillators (2) in the form of (1) and briefly review previous approaches used for simulating these systems in visual computing. In Sect. 3, we describe the exponential Rosenbrock methods as an alternative approach for solving large stiff systems (1). The implementation of these methods is discussed in Sect. 4, where we also introduce a new procedure to further improve one of the state-of-the-art algorithms. In Sect. 5 we demonstrate the efficiency of the exponential Rosenbrock methods on a number of complex models in visual computing. In particular, we address the simulation of deformable bodies, fibers including elastic collisions, and crash scenarios including nonelastic deformations. These examples focus on relevant aspects in the realm of visual computing, like stability and energy conservation, large stiffness values, and high fidelity and visual accuracy. We include an evaluation against classical and state-of-the-art methods used in this field. Finally, some concluding remarks are given in Sect. 6.

2 Reformulation of Systems of Coupled Oscillators

We first consider the system of coupled oscillators (2). Let $x(t) \in \mathbb{R}^{3N}$, $M \in \mathbb{R}^{3N \times 3N}$, $D \in \mathbb{R}^{3N \times 3N}$, $K \in \mathbb{R}^{3N \times 3N}$ and $g(x) \in \mathbb{R}^{3N}$ denote the vector of positions, the mass matrix (often diagonal and thus nonsingular), the damping matrix, the spring matrix (stiff), and the total external forces acting on the system, respectively. Using these matrix notations and denoting $A = M^{-1}K$, (2) can be written as a system of second-order ODEs

$$x''(t) + Ax(t) = g(x(t)), \quad x(t_0) = x_0, \quad x'(t_0) = v_0. \quad (3)$$

Here x_0, v_0 are some given initial positions and velocities. For simplicity we neglect damping and assume that A is a symmetric, positive definite matrix (this is a reasonable assumption in many models, see [38]). Therefore, there exists a unique positive definite matrix Ω such that $A = \Omega^2$ (and clearly Ω^{-1} exists).

Following our approach in [40], we introduce the new variable

$$u(t) = \begin{bmatrix} \Omega x(t) \\ x'(t) \end{bmatrix}. \quad (4)$$

Using this one can reformulate (3) as a first-order system of ODEs of the form like 92
 (1): 93

$$u'(t) = F(u(t)) = \mathcal{A}u(t) + G(u(t)), \quad u(t_0) = u_0, \quad (5)$$

where 94

$$\mathcal{A} = \begin{bmatrix} \mathbf{0} & \Omega \\ -\Omega & \mathbf{0} \end{bmatrix}, \quad G(u) = \begin{bmatrix} \mathbf{0} \\ g(x) \end{bmatrix}. \quad (6)$$

Since the linear spring forces usually possess high frequencies (thus $\|K\| \gg 1$ and 95
 so is $\|A\|$), (5) becomes a very stiff ODE. Regarding the new formulation (5)–(6), 96
 we observe the following two remarks. 97

Remark 1 Clearly, the new linear part associated with \mathcal{A} , that is a skew-symmetric 98
 matrix. We note that this significantly differs from the common way of reformulating 99
 (3) that is to use the change of variable $X(t) = [x(t), x'(t)]^T$ which 100
 results in a non-symmetric matrix. The advantage here is that since \mathcal{A} is a skew- 101
 symmetric matrix, its nonzero eigenvalues are all pure imaginary and are in pairs 102
 $\pm\lambda_k i$. We also observe that \mathcal{A} is an infinitesimal symplectic (or Hamiltonian). This 103
 is because, by definition of an infinitesimal symplectic matrix, we check whether 104
 $W\mathcal{A} + \mathcal{A}^T W = \mathbf{0}$, where W is the anti-symmetric matrix $W = \begin{bmatrix} \mathbf{0} & I \\ -I & \mathbf{0} \end{bmatrix}$. This 105
 can be easily verified since 106

$$W\mathcal{A} = \begin{bmatrix} -\Omega & \mathbf{0} \\ \mathbf{0} & -\Omega \end{bmatrix},$$

which is clearly a symmetric matrix, i.e., $W\mathcal{A} = (W\mathcal{A})^T$. 107

Remark 2 If the Jacobian matrix $F'(u) = \mathcal{A} + G'(u)$ is infinitesimal symplectic, 108
 (5) is a Hamiltonian system. This can be fulfilled since a typical situation in 109
 Hamiltonian systems is that $g(x) = \nabla f(x)$ for some function $f(x)$ and thus 110
 $g'(x) = \nabla^2 f(x)$ becomes a Hessian matrix, which is symmetric. 111

As seen, either using the common way (mentioned in Remark 1) or the new way 112
 (4) for reformulating (3), one has to solve the stiff ODE (5). In visual computing 113
 it is usually solved by explicit methods such as the fourth-order Runge–Kutta 114
 methods, semi-implicit methods such as the Störmer–Verlet methods, the backward 115
 differentiation formulas (BDF-1 and BDF-2) methods, or IMEX methods. In this 116
 regard, we refer to some contributions in the context of interacting deformable 117
 bodies, cloth, solids, and elastic rods, see [3, 4, 12, 16, 19, 47]. For large-scale 118
 applications associated with stiff systems, however, both types of these time 119
 integration techniques have their own limitations as mentioned in the introduction. 120
 In recent years, exponential integrators have shown to be competitive for large- 121
 scale problems in physics and for nonlinear parabolic PDEs, as well as for highly 122

oscillatory problems (see [24]). They have attracted much attention by the broad 123
 computational mathematics community since mid-1990s. At the time while solving 124
 linear systems $(I - \alpha h J)x = v$ with some Jacobian matrix J (required when 125
 using implicit methods) is generally only of linear convergence, it was realized that 126
 Krylov subspace methods for approximating the action of a matrix exponential on a 127
 vector, $e^{hJ}v$, offer superlinear convergence (see [21]). Unless a good preconditioner 128
 is available, this is clearly a computational advantage of exponential integrators 129
 over implicit methods. This has been addressed in the visual computing community 130
 very recently through a number of interesting work on exponential integrators, 131
 see e.g.[37–40]. Inspired by this interest, in the following sections we will show 132
 how exponential Rosenbrock methods—one of the popular classes of exponential 133
 integrators—can be applied for simulating systems of coupled oscillators. 134

3 Explicit Exponential Rosenbrock Methods

135

In this section, based on [23, 26, 29, 32, 34] we present a compact summary 136
 of the introduction of exponential Rosenbrock methods and their derivations for 137
 methods of order up to 5. We then display some efficient schemes for our numerical 138
 experiments for some applications in visual computing. 139

3.1 Approach

140

Motivated by the idea of deriving Rosenbrock-type methods, see [18, Chap. IV.7], 141
 instead of integrating the fully nonlinear system (1) (which has a large nonlinearity 142
 for stiff problems), one can replace it by a sequence of semilinear problems 143

$$u'(t) = F(u(t)) = J_n u(t) + g_n(u(t)), \quad (7)$$

by linearizing the forcing term $F(u)$ in each time step at the numerical solution u_n 144
 (due to [42]) with 145

$$J_n = F'(u_n), \quad g_n(u) = F(u) - J_n u \quad (8)$$

are the Jacobian and the nonlinear remainder, respectively. An advantage of this 146
 approach is that $g'_n(u_n) = F'(u_n) - J_n = 0$ which shows that the new nonlinearity 147
 $g_n(u)$ has a much smaller Lipschitz constant than that of the original one $F(u)$. 148
 The next idea is to handle the stiffness by solving the linear part $J_n u$ exactly and 149
 integrating the new nonlinearity $g_n(u)$ explicitly. For that, the representation of the 150
 exact solution at time $t_{n+1} = t_n + h$ of (7) using the variation-of-constants formula 151

$$u(t_{n+1}) = e^{hJ_n} u(t_n) + \int_0^h e^{(h-\tau)J_n} g_n(u(t_n + \tau)) d\tau \quad (9)$$

plays a crucial role in constructing this type of integrators. As seen from (9), while the linear part can be integrated exactly by computing the action of the matrix exponential e^{hJ_n} on the vector $u(t_n)$, the integral involving $g_n(u)$ can be approximated by some quadrature. This procedure results in the so-called *exponential Rosenbrock methods*, see [23, 26].

Remark 3 For the system of coupled oscillators (2), the forcing term $F(u)$ has the semilinear form (5), which can be considered as a fixed linearization. Therefore, one can directly apply explicit the exponential Runge–Kutta methods (see [22]) to (5). The advantage of these methods is that the time-step h is not restricted by the CFL condition when integrating the linear part $\mathcal{A}u$. In our applications, however, the nonlinearity $G(u)$ is large in which the CFL condition usually serves as a reference for setting the time-step. In particular, for the stability hL_G should be sufficiently small (L_G is the Lipschitz constant of $G(u)$). In this regard, the dynamic linearization approach (7) applied to (5)

$$u'(t) = F(u) = \mathcal{A}u + G(u) = J_n u + G_n(u) \quad (10)$$

with

$$J_n = \mathcal{A} + G'(u_n), \quad (11)$$

offers a great advantage in improving the stability (in each step) when integrating $G(u)$. This is because instead of integrating the original semilinear problem with large nonlinearity $G(u)$, we only have to deal with a much smaller nonlinearity $G_n(u)$ (as mentioned above). Note that the new linear part $J_n u$ with the Jacobian J_n now incorporates both \mathcal{A} and the Jacobian of the nonlinearity $G(u)$, which can be again solved exactly. It is thus anticipated that this idea of exponential Rosenbrock methods opens up the possibility to take even larger time steps compared to exponential Runge–Kutta methods.

3.2 Formulation of a Second-Order and General Schemes

In this subsection, we will illustrate the approach of exponential Rosenbrock methods by presenting a simple derivation of a second-order scheme and formulating general schemes.

3.2.1 A Second-Order Scheme

First, expanding $u(t_n + \tau)$ in a Taylor series gives $u(t_n + \tau) = u(t_n) + \tau u'(t_n) + O(\tau^2)$. Then inserting this into $g_n(u(t_n + \tau))$ and again expanding it as a Taylor series

around $u(t_n)$ (using $g'_n(u(t_n)) = 0$) leads to

181

$$g_n(u(t_n + \tau)) = g_n(u(t_n)) + O(\tau^2). \quad (12)$$

Inserting (12) into the integral of (9) and denoting $\varphi_1(hJ_n) = \frac{1}{h} \int_0^h e^{(h-\tau)J_n} d\tau$ gives

182

$$u(t_{n+1}) = e^{hJ_n} u(t_n) + h\varphi_1(hJ_n)g_n(u(t_n)) + O(h^3). \quad (13)$$

Neglecting the local error term $O(h^3)$ results in a second-order scheme, which can be reformulated as

183

184

$$u_{n+1} = u_n + h\varphi_1(hJ_n)F(u_n) \quad (14)$$

by replacing $g_n(u(t_n))$ by (8) and using the fact that $\varphi_1(z) = (e^z - 1)/z$. This scheme was derived before and named as *exponential Rosenbrock-Euler method*, see [23, 26] (since when considering the formal limit $J_n \rightarrow \mathbf{0}$, (14) is the underlying Euler method). The derivation here, however, shows directly that this scheme has an order of consistency three and thus it is a second-order stiffly accurate method (since the constant behind the Landau notation \mathcal{O} only depends on the regularity assumptions on $u(t)$ and $g_n(u)$, but is independent of $\|J_n\|$).

185

186

187

188

189

190

191

3.2.2 General Schemes

192

For the derivation of higher-order schemes, one can proceed in a similar way as for the construction of classical Runge–Kutta methods. Namely, one can approximate the integral in (9) by using some higher-order quadrature rule with nodes c_i in $[0, 1]$ and weights $b_i(hJ_n)$ which are matrix functions of hJ_n , yielding

193

194

195

196

$$u(t_{n+1}) \approx e^{hJ_n} u(t_n) + h \sum_{i=1}^s b_i(hJ_n)g_n(u(t_n + c_i h)). \quad (15)$$

The unknown intermediate values $u(t_n + c_i h)$ can be again approximated by using (9) (with $c_i h$ in place of h) with another quadrature rule using the same nodes c_j , $1 \leq j \leq i-1$, (to avoid generating new unknowns) and new weights $a_{ij}(hJ_n)$, leading to

197

198

199

200

$$u(t_n + c_i h) \approx e^{c_i h J_n} u(t_n) + h_n \sum_{j=1}^{i-1} a_{ij}(hJ_n)g_n(u(t_n + c_j h)). \quad (16)$$

Let us denote $u_n \approx u(t_n)$ and $U_{ni} \approx u(t_n + c_i h_n)$. As done for (14), using (12) (with $c_i h$, h in place of τ , respectively) one can reformulate (15) and (16) in a similar manner, which yields the general format of s -stage explicit exponential Rosenbrock

201

202

203

methods

204

$$U_{ni} = u_n + c_i h \varphi_1(c_i h J_n) F(u_n) + h \sum_{j=2}^{i-1} a_{ij}(h J_n) D_{nj}, \quad (17a)$$

$$u_{n+1} = u_n + h \varphi_1(h J_n) F(u_n) + h \sum_{i=2}^s b_i(h J_n) D_{ni} \quad (17b)$$

with

205

$$D_{ni} = g_n(U_{ni}) - g_n(u_n), \quad (17c)$$

As in (12), we have $D_{ni} = O(h^2)$. Thus, the general methods (17) are small perturbations of the exponential Rosenbrock–Euler method (14). Note that the weights $a_{ij}(h J_n)$ and $b_i(h J_n)$ are usually linear combinations of $\varphi_k(c_i h J_n)$ and $\varphi_k(h J_n)$, respectively, where the φ functions (similar to φ_1) are given by

$$\varphi_k(hZ) = \frac{1}{h^k} \int_0^h e^{(h-\tau)Z} \tau^{k-1} d\tau, \quad k \geq 1 \quad (18)$$

and satisfy the recursion relation

210

$$\varphi_{k+1}(z) = \frac{\varphi_k(z) - \frac{1}{k!}}{z}, \quad k \geq 1. \quad (19)$$

It is important to note that these functions are bounded (uniformly) independently of $\|J_n\|$ (i.e. the stiffness) so are the coefficients $a_{ij}(h J_n)$ and $b_i(h J_n)$ (see e.g. [24]).

Clearly, using exponential Rosenbrock schemes (17) offers some good advantages. First, they do not require the solution of linear or nonlinear systems of equations. Second, as mentioned above, they offer a better stability when solving stiff problems with large nonlinearities and thus allow to use larger time-steps. Third, since the Jacobian of the new nonlinearity vanishes at every step ($g'_n(u_n) = 0$), the derivation of the order conditions and hence the schemes can be simplified considerably. In particular, higher-order stiffly accurate schemes can be derived with only a few stages (see the next section).

The convergence analysis of exponential Rosenbrock methods is usually carried out in an appropriate framework (strongly continuous semigroup) under regularity assumptions on the solution $u(t)$ (sufficiently smooth) and $g_n(u)$ (sufficiently Fréchet differentiable in a neighborhood of the solution) with uniformly bounded derivatives in some Banach space. For more details, we refer to [26, 32].

225

3.3 Selected Schemes for Numerical Simulations

226

First, we discuss some important points for the derivation of exponential Rosenbrock schemes. Clearly, the unknown coefficients $a_{ij}(hJ_n)$ and $b_i(hJ_n)$ have to be determined by solving order conditions. For nonstiff problems, where the Jacobian matrix has a small norm, one can expand those matrix functions using classical Taylor series expansions, leading to nonstiff order conditions and in turn classical exponential schemes (see e.g. [9, 27]). For stiff problems, however, one has to be cautious when analyzing the local error to make sure that error terms do not involve powers of J_n (which has a large norm). Recently, Luan and Ostermann [30, 33] derived a new expansion of the local error which fulfills this requirement and thus derived a new stiff order conditions theory for methods of arbitrary order (both for exponential Runge–Kutta and exponential Rosenbrock methods). As expected, with the same order, the number of order conditions for exponential Rosenbrock methods is significant less than those for exponential Runge–Kutta methods. For example, in Table 1, we display the required 4 conditions for deriving schemes up to order 5 in [32] (note that for exponential Runge–Kutta methods, 16 order conditions are required for deriving schemes of order 5, see [31]).

We note that with these order conditions one can easily derive numerous different schemes of order up to 5. Taking the compromise between efficiency and accuracy into consideration, we seek for the most efficient schemes for our applications. Namely, the following two representative fourth-order schemes are selected.

`exprb42` (a fourth-order 2-stage scheme which can be considered as a superconvergent scheme, see [29]):

$$U_{n2} = u_n + \frac{3}{4}h\varphi_1(\frac{3}{4}hJ_n)F(u_n), \quad (20a)$$

$$u_{n+1} = u_n + h\varphi_1(hJ_n)F(u_n) + h\frac{32}{9}\varphi_3(hJ_n)(g_n(U_{n2}) - g_n(u_n)). \quad (20b)$$

Table 1 Stiff order conditions for exponential Rosenbrock methods up to order five. Here Z and K denote arbitrary square matrices and $\psi_{3,i}(z) = \sum_{k=2}^{i-1} a_{ik}(z) \frac{c_i^k}{2^k} - c_i^3 \varphi_3(c_i z)$

No.	Order condition	Order	
1	$\sum_{i=2}^s b_i(Z) c_i^2 = 2\varphi_3(Z)$	3	t3.1
2	$\sum_{i=2}^s b_i(Z) c_i^3 = 6\varphi_4(Z)$	4	t3.2
3	$\sum_{i=2}^s b_i(Z) c_i^4 = 24\varphi_5(Z)$	5	t3.3
4	$\sum_{i=2}^s b_i(Z) c_i K \psi_{3,i}(Z) = 0$	5	t3.4
			t3.5

pexprb43 (a fourth-order 3-stage scheme, which can be implemented in 249 parallel, see [34]): 250

$$U_{n2} = u_n + \frac{1}{2}h\varphi_1(\frac{1}{2}hJ_n)F(u_n), \quad (21a)$$

$$U_{n3} = u_n + h\varphi_1(hJ_n)F(u_n), \quad (21b)$$

$$\begin{aligned} u_{n+1} = u_n + h\varphi_1(hJ_n)F(u_n) + h\varphi_3(hJ_n)(16D_{n2} - 2D_{n3}) \\ + h\varphi_4(hJ_n)(-48D_{n2} + 12D_{n3}). \end{aligned} \quad (21c)$$

Note that the vectors D_{n2} and D_{n3} in (21) are given by (17c), i.e., $D_{n2} = g_n(U_{n2}) - 251$
 $g_n(u_n)$ and $D_{n3} = g_n(U_{n3}) - g_n(u_n)$. 252

4 Implementation

253

In this section, we present the implementation of exponential Rosenbrock methods 254 for the new formulation (5) of the system of coupled oscillators. First, we discuss 255 on the computation of the matrix square root Ω needed for the reformulation. We 256 then briefly review some state-of-the-art algorithms for implementing exponential 257 Rosenbrock methods and introduce a new routine which is an improved version 258 of one of these algorithms (proposed very recently in [35]) for achieving more 259 efficiently. Finally, we specifically discuss applying this routine for implementing 260 the selected schemes exprb42 and pexprb43. 261

4.1 Computation of the Matrix Square Root $\Omega = \sqrt{A}$

262

For the computation of $\Omega = \sqrt{A}$ used in (5), we follow our approach in [40]. 263 Specifically, we use the Schur decomposition for moderate systems. For large 264 systems, the Newton square root iteration (see [20]) is employed in order to avoid an 265 explicit precomputation of Ω . Namely, one can use the following simplified iteration 266 method for approximating the solution of the equation $\Omega^2 = A$: 267

- (i) choose $\Omega_0 = A$ ($k = 0$), 268
- (ii) update $\Omega_{k+1} = \frac{1}{2}(\Omega_k + \Omega_k^{-1}A)$. 269

This method offers unconditional quadratic convergence with much less cost compared to the Schur decomposition. We note that Ω^{-1} can be computed efficiently 270 using a Cholesky decomposition since Ω is symmetric and positive definite and it 271 is given by $\Omega^{-1} = \mathbf{S}^{-1}\mathbf{S}^{-T}$, where \mathbf{S} is an upper triangular matrix with real and 272 positive diagonal entries. For more details, we refer to [20, 40]. 273

274

With Ω at hand, one can easily compute the Jacobian J_n as in (11) and ²⁷⁵ $F(u)$, $G_n(u)$ as in (10). As the next step, we discuss the implementation of the ²⁷⁶ exponential Rosenbrock schemes. ²⁷⁷

4.2 Implementation of Exponential Rosenbrock Methods

278

In view of the exponential Rosenbrock schemes in Sect. 3, each stage requires ²⁷⁹ the evaluation of a linear combination of φ -functions acting on certain vectors ²⁸⁰ v_0, \dots, v_p ²⁸¹

$$\varphi_0(M)v_0 + \varphi_1(M)v_1 + \varphi_2(M)v_2 + \dots + \varphi_p(M)v_p, \quad (22)$$

where the matrix M here could be $h J_n$ or $c_i h J_n$. Starting from a seminal contribution ²⁸² by Hochbruck and Lubich [21] (which they analyzed Krylov subspace methods for ²⁸³ efficiently computing the action of a matrix exponential (with a large norm) on some ²⁸⁴ vector), many more efficient techniques have been proposed. A large portion of ²⁸⁵ these developments is concerned with computing the expression (22). For example, ²⁸⁶ we mention some of the state-of-the-art algorithms: `expmv` proposed by Al-Mohy ²⁸⁷ and Higham in [1] (using a truncated standard Taylor series expansion), `phipm` ²⁸⁸ proposed by Niessen and Wright in [41] (using adaptive Krylov subspace methods), ²⁸⁹ and `explaja` proposed by Caliari et al. in [5, 6] (using Leja interpolation). With ²⁹⁰ respect to computational time, it turns out that `phipm` offers an advantage. This ²⁹¹ algorithm utilizes an adaptive time-stepping method to evaluate (22) using only ²⁹² one matrix function (see Sect. 4.2.1 below). This task is carried out in a lower ²⁹³ dimensional Krylov subspace using standard Krylov subspace projection methods ²⁹⁴ i.e. the Arnoldi iteration. Moreover, the dimension of Krylov subspaces and the ²⁹⁵ number of substeps are also chosen adaptively for improving efficiency. ²⁹⁶

Recently, the `phipm` routine was modified by Gaudreault and Pudykiewicz in ²⁹⁷ [13] (Algorithm 2) by using the incomplete orthogonalization method (IOM) within ²⁹⁸ the Arnoldi iteration and by adjusting the two crucial initial parameters for starting ²⁹⁹ the Krylov adaptivity. This results in the new routine called `phipm/IOM2`. It is ³⁰⁰ shown in [13] that this algorithm reduces computational time significantly compared ³⁰¹ to `phipm` when integrating the shallow water equations on the sphere. ³⁰²

Very recently, the authors of [35] further improved `phipm/IOM2` which resulted ³⁰³ in a more efficient routine named as `phipm_simul_iom2`. For the reader's ³⁰⁴ convenience, we present the idea of the adaptive time-stepping method (originally ³⁰⁵ proposed in [41]) for evaluating (22) and introduce some new features of the new ³⁰⁶ routine `phipm_simul_iom2`. ³⁰⁷

4.2.1 Computing of Linear φ -Combinations Based on Time-Stepping

308

It was observed that the following linear ODE

309

$$u'(t) = Mu(t) + v_1 + tv_2 + \cdots + \frac{t^{p-1}}{(p-1)!}v_p, \quad u(0) = v_0, \quad (23)$$

defined on the interval $[0, 1]$ has the exact solution at $t = 1, u(1)$ to be the expression (22). The time-stepping technique approximates $u(1)$ by discretizing $[0, 1]$ into subintervals $0 = t_0 < t_1 < \cdots < t_k < t_{k+1} = t_k + \tau_k < \cdots < t_K = 1$ with a substepsize sequence τ_k ($k = 0, 1, \dots, K-1$) and using the following relation between $u(t_{k+1})$ and its previous solution $u(t_k)$:

$$u(t_{k+1}) = \varphi_0(\tau_k M)u(t_k) + \sum_{i=1}^p \tau_k^i \varphi_i(\tau_k M) \sum_{j=0}^{p-i} \frac{t_k^j}{j!} v_{i+j}. \quad (24)$$

Using the recursion relation (19) and (24) can be simplified as

315

$$u(t_{k+1}) = \tau_k^p \varphi_p(\tau_k M)w_p + \sum_{j=0}^{p-i} \frac{t_k^j}{j!} w_j, \quad (25)$$

where the vectors w_j satisfy the recurrence relation

$$w_0 = u(t_k), \quad w_j = Mw_{j-1} + \sum_{\ell=0}^{p-j} \frac{t_k^\ell}{\ell!} v_{j+\ell}, \quad j = 1, \dots, p. \quad (26)$$

Equation (25) implies that evaluating $u(t_K) = u(1)$ i.e. the expression (22) requires only one matrix function $\varphi_p(\tau_k M)w_p$ in each substep instead of $(p+1)$ matrix-vector multiplications. As $0 < \tau_k < 1$, this task can be carried out in a Krylov subspace of lower dimension m_k , and in each substep only one Krylov projection is needed. With a reasonable number of substeps K , it is thus expected that the total computational cost of $O(m_1^2) + \cdots + O(m_K^2)$ for approximating $\varphi_p(\tau_k M)w_p$ is less than that of $O(m^2)$ for approximating $\varphi_p(M)v$ in a Krylov subspace of dimension m . If K is too large (e.g. when the spectrum of M is very large), this might be not true. This case, however, is handled by using the adaptive Krylov algorithm in [41] allowing to adjust both the dimension m and the step sizes τ_k adaptivity. This explains the computational advance of this approach compared to standard Krylov algorithms.

4.2.2 New Routine `phipm_simul_iom2` [35]

329

First, we note that the resulting routine `phipm_simul_iom2` optimizes computational aspects of `phipm/IOM2` corresponding to the following two specific changes: 330
331
332

1. Unlike (22), where each of the φ_k functions is evaluated at the same argument M , the internal stages of exponential Rosenbrock schemes require evaluating the φ functions at fractions of the matrix M : 333
334
335

$$w_k = \sum_{l=1}^p \varphi_l(c_k M) v_l, \quad k = 2, \dots, s, \quad (27)$$

where now the node values c_2, \dots, c_s are scaling factors used for each v_k 336 output. To optimize this evaluation, `phipm_simul_iom2` computes all w_k 337 outputs in (27) simultaneously, instead of computing only one at a time. This 338 is accomplished by first requiring that the entire array c_2, \dots, c_s as an input to 339 the function. Within the substepping process (24), each value c_j is aligned with 340 a substep-size τ_k . The solution vector is stored at each of these moments and 341 on output the full set $\{w_k\}_{k=1}^s$ is returned. Note that this approach is similar but 342 differs from [48] that it guarantees no loss of solution accuracy since it explicitly 343 stops at each c_k instead of using interpolation to compute w_k as in [48]. 344

2. In view of the higher-order exponential Rosenbrock schemes (see also from 345 Sect. 3.3), it is realized that they usually use a subset of the φ_l functions. Therefore, 346 multiple vectors in (27) will be zero. In this case, `phipm_simul_iom2` 347 will check whether $w_{j-1} \neq 0$ (within the recursion (26)) before computing 348 the matrix-vector product $M w_{j-1}$. While matrix-vector products require $O(n^2)$ 349 work, checking $u \neq 0$ requires only $O(n)$. This can result in significant savings 350 for large n . 351

4.2.3 Implementation of `exprb42` and `pexprb43`

352

Taking a closer look at the structures of the two selected exponential Rosenbrock 353 schemes `exprb42` and `pexprb43`, we now make use of `phipm_simul_iom2` 354 for implementing these schemes. For simplicity, let us denote $M = hJ_n$ and $v = 355$
 $hF(u_n)$. 356

Implementation of `exprb42`: Due to the structure of `exprb42` given in (20), one 357 needs two calls to `phipm_simul_iom2`: 358

1. Evaluate $y_1 = \varphi_1(\frac{3}{4}M)w_1$ with $w_1 = \frac{3}{4}v$ (so $w_0 = 0$) to get $U_{n2} = u_n + y_1$, 359
2. Evaluate $w = \varphi_1(M)v_1 + \varphi_3(M)v_3$ (i.e. $v_0 = v_2 = 0$) with $v_1 = v$, $v_3 = 360$
 $\frac{32}{9}hD_{n2}$ to get $u_{n+1} = u_n + w$. 361

Implementation of pexprb43: Although pexprb43 is a 3-stage scheme, its special structure (21) allows to use only two calls to phipm_simul_iom2: 362
363

1. Evaluate both terms $y_1 = \varphi_1(\frac{1}{2}M)v$ and $z_1 = \varphi_1(M)v$ simultaneously to get the two stages $U_{n2} = u_n + \frac{1}{2}y_1$ and $U_{n3} = u_n + z_1$, 364
365
2. Evaluate $w = \varphi_3(M)v_3 + \varphi_4(M)v_4$ (i.e. $v_0 = v_1 = v_2 = 0$) with $v_3 = h(16D_{n2} - 2D_{n3})$, $v_4 = h(-48D_{n2} + 12D_{n3})$ to get $u_{n+1} = U_{n3} + w$. 366
367

5 Numerical Examples

368

In this section we present several numerical examples to study the behavior of the presented exponential Rosenbrock-type methods, in particular the fourth-order scheme exprb42 using two stages and the fourth-order pexprb43 scheme using three stages implemented in parallel. 369
370
371
372

In particular, we focus on relevant aspects in the realm of visual computing, like stability and energy conservation, large stiffness, and high fidelity and visual accuracy. A tabular summary of the models that are used throughout this section can be found in Table 2. Furthermore, our simulation includes important aspects like elastic collisions and nonelastic deformations. The presented exponential Rosenbrock-type methods are evaluated against classical and state-of-the-art methods used in visual computing, in particular against the implicit-explicit variational (IMEX) integrator (cf. [44, 45]), the standard fourth-order Runge–Kutta method (see [28, 43]), and the implicit BDF-1 integrator (see [11]). All simulation results visualized here have been computed using a machine with an Intel(R) Xeon E5 3.5 GHz and 32 GB DDR-RAM. For each simulation scenario the largest possible time step size is used which still leads to a desired visually plausible result. 373
374
375
376
377
378
379
380
381
382
383
384

5.1 Simulation of Deformable Bodies

385

In order to illustrate the accurate energy preservation of the presented exponential Rosenbrock-type methods, we set up an undamped scene of an oscillating coil spring, which is modeled as a deformable body composed of tetrahedra, in particular of 8000 vertices corresponding to $N = 24\,000$ equations of motion, which are derived from a system of coupled oscillators with uniform spring stiffness of $k = 10^6$. Since the coil spring is exposed to an external forces field, it starts to oscillate as illustrated in Fig. 1. It can be seen that the top of the coil spring returns to its initial height periodically during the simulation which can be seen as an indicator for energy conservation. In fact when using the exponential Rosenbrock-type methods exprb42 and pexprb43 we observe that the discrete energy is only slightly oscillating around the real energy without increasing oscillations over time. In contrast, the standard fourth order Runge–Kutta method respectively the BDF-1 386
387
388
389
390
391
392
393
394
395
396
397

Table 2 Overview of the test cases used for the numerical experiments. Their complexity N (i.e. the number of the resulting equations of motion), the simulated time, and respective running times for the exponential Rosenbrock-type methods `exprb42` and `pexprb43`, the implicit-explicit variational integrator (V-IMEX), the standard fourth order Runge–Kutta method (RK4), and the BDF-1 integrator are shown

No.	Model	N	Sim. time	<code>exprb42</code>	<code>pexprb43</code>	V-IMEX	RK 4	BDF-1
16.1	1	24k	60 s	55 s	47 s	12 min	46 min	62 min
16.2	Coil Spring							
16.3	2	90k	15 s	52 s	51 s	11 min	53 min	72 min
16.4	Brushing							
16.5	3	360k	2 s	44 s	44 s	9 min	47 min	58 min
	Crash test (moderate)							
4	4	360k	2 s	47 s	46 s	9 min	47 min	59 min
	Crash test (fast)							

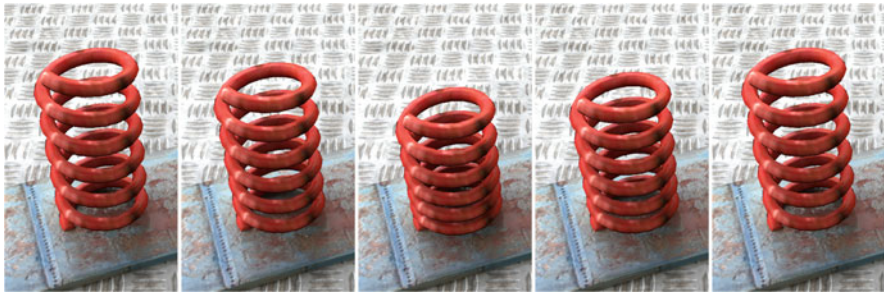


Fig. 1 Simulation of an oscillating coil spring

integrator generate significant numerical viscosity leading to a loss of energy around 398
22% respectively 40% after 60 s of simulated time. 399

The exponential Rosenbrock-type methods `exprb42` and `pexprb43` show 400
their advantageous behavior since these methods can be applied with orders of 401
magnitude larger time steps compared to the other integrators. Even with a step 402
size of $h = 0.05$ the relative error is still below 2% for `exprb42` and about a single 403
percent for `pexprb43`.¹ From a point of view of computation time, we achieve 404
a speed up of a factor of around thirteen using `exprb42` and of over fifteen using 405
`pexprb43` compared to the second best method, the variational IMEX integrator as 406
illustrated in Table 2. Compared to the other methods, the exponential Rosenbrock- 407
type methods allow for accurate simulations in real-time. 408

5.2 Simulation of Fibers Including Elastic Collisions

Fibers are canonical examples for complex interacting systems. According to the 410
work of Michels et al. (see [39]), we set up a toothbrush composed of individual 411
bristles. Each bristle consists of coupled oscillators that are connected in such a 412
way that the fiber axis is enveloped by a chain of cuboid elements. For preventing 413
a volumetric collapse during the simulation, additional diagonal springs are used. 414
The toothbrush consists of 1500 bristles, each of 20 particles leading to 90 000 415
equations of motion. We make use of additional repulsive springs in order to 416
prevent from interpenetrations.² Since the approach allows for the direct use of 417
realistic parameters in order to set up the stiffness values in the system of coupled 418
oscillators, we employ a Young's modulus of $3.2 \cdot 10^6 \text{ Ncm}^{-2}$, a torsional modulus 419
of 10^5 Ncm^{-2} , and segment thicknesses of 0.12 mm. 420

¹We estimated the error after 60 s of simulated time based on the accumulated Euclidean distances of the individual particles in the position space compared to ground truth values which are computed with a sufficiently small step size.

²In order to detect collisions efficiently, we make use of a standard bounding volume hierarchy.



Fig. 2 Simulation of a brush cleaning a bronze-colored paperweight



Fig. 3 Simulations of two frontal nonelastic crash scenarios: a car with moderate velocity (top) and high velocity (bottom)

We simulate 15 s of a toothbrush cleaning a paperweight illustrated in Fig. 2. This 421 simulation can be carried out almost in real-time which is not possible with the use 422 of classical methods as illustrated in Table 2. 423

5.3 Crash Test Simulation Including Nonelastic Deformations

As a very complex example with relevance in the context of special effects, we 425 simulate a frontal crash of a car into a wall as illustrated in Fig. 3. The mesh of the 426 car and its interior is composed of 120 000 vertices leading to 360 000 equations of 427 motion. The global motion (i.e. the rebound of the car) is computed by treating the 428 car as a rigid body. Using an appropriate bounding box, this can be easily carried out 429 in real-time. The deformation is then computed using a system of coupled oscillators 430 with structural stiffness values of $k = 10^4$ and bending stiffness values of $k/100$. If 431 the deformation reaches a defined threshold, the rest lengths of the corresponding 432 springs are corrected in a way, that they do not elastically return to their initial 433 shape. Using the exponential Rosenbrock-type methods, the whole simulation can 434 be carried out at interactive frame rates. Such an efficient computation can not be 435 achieved with established methods as illustrated in Table 2. 436

6 Conclusion

437

We introduced the class of *explicit exponential Rosenbrock methods* for the time 438
 integration of large systems of nonlinear differential equations. In particular, the 439
 exponential Rosenbrock-type fourth-order schemes `exprb42` using two stages 440
 and `pexprb43` using three stages were discussed and their implementation 441
 were addressed. In order to study their behavior, a broad spectrum of numerical 442
 examples was computed. In this regard, the simulation of deformable bodies, fibers 443
 including elastic collisions, and crash scenarios including nonelastic deformations 444
 was addressed focusing on relevant aspects in the realm of visual computing, like 445
 stability and energy conservation, large stiffness values, and high fidelity and visual 446
 accuracy. An evaluation against classical and state-of-the-art methods was presented 447
 demonstrating their superior performance with respect to the simulation of large 448
 systems of stiff differential equations. 449

Acknowledgments The first author is partially supported by NSF grant DMS–2012022. The sec- 450
 ond author has been partially supported by King Abdullah University of Science and Technology 451
 (KAUST baseline funding). 452

References

453

1. A.H. Al-Mohy, N.J. Higham, Computing the action of the matrix exponential, with an 454
 application to exponential integrators. *SIAM J. Sci. Comput.* **33**, 488–511 (2011) 455

2. U. Ascher, S. Ruuth, B. Wetton, Implicit-explicit methods for time-dependent PDEs. *SIAM J. 456
 Numer. Anal.* **32**(3), 797–823 (1997) 457

3. D. Baraff, A. Witkin, Large steps in cloth simulation, in *ACM Transactions on Graphics, 458
 SIGGRAPH'98* (ACM, New York, 1998), pp. 43–54 459

4. M. Bergou, M. Wardetzky, S. Robinson, B. Audoly, E. Grinspan, Discrete elastic rods. *ACM 460
 Trans. Graph.* **27**(3), 63:1–63:12 (2008) 461

5. M. Caliari, A. Ostermann, Implementation of exponential Rosenbrock-type integrators. *Appl. 462
 Numer. Math.* **59**(3–4), 568–581 (2009) 463

6. M. Caliari, P. Kandolf, A. Ostermann, S. Rainer, The Leja method revisited: backward error 464
 analysis for the matrix exponential. *SIAM J. Sci. Comput.* **38**(3), A1639–A1661 (2016) 465

7. W.L. Chao, J. Solomon, D. Michels, F. Sha, Exponential integration for Hamiltonian Monte 466
 Carlo, in *Proceedings of the 32nd International Conference on Machine Learning*, ed. by 467
 F. Bach, D. Blei. *Proceedings of Machine Learning Research*, vol. 37, pp. 1142–1151 (PMLR, 468
 Lille, 2015) 469

8. Y.J. Chen, U. Ascher, D. Pai, Exponential Rosenbrock-Euler integrators for elastodynamic 470
 simulation. *IEEE Trans. Visual. Comput. Graph.* (2017) 471

9. S.M. Cox, P.C. Matthews, Exponential time differencing for stiff systems. *J. Comput. Phys.* 472
176(2), 430–455 (2002) 473

10. C. Curtiss, J.O. Hirschfelder, Integration of stiff equations. *Proc. Natl. Acad. Sci.* **38**(3), 235– 474
 243 (1952) 475

11. C.F. Curtiss, J.O. Hirschfelder, Integration of stiff equations. *Proc. Natl. Acad. Sci. USA* **38**(3), 476
 235–243 (1952) 477

AQ3

12. B. Eberhardt, O. Etzmüller, M. Hauth, Implicit-explicit schemes for fast animation with particle systems, in *Proceedings of the 11th Eurographics Workshop on Computer Animation and Simulation (EGCAS)* (Springer, Berlin, 2000), pp. 137–151 479
480

13. S. Gaudreault, J. Pudykiewicz, An efficient exponential time integration method for the numerical solution of the shallow water equations on the sphere. *J. Comput. Phys.* **322**, 827–848 (2016) 481
482
483

14. C. Gear, *Numerical Initial Value Problems in Ordinary Differential Equations* (Prentice-Hall, Englewood Cliffs, 1971) 484
485

15. S. Geiger, G. Lord, A. Tambue, Exponential time integrators for stochastic partial differential equations in 3D reservoir simulation. *Comput. Geosci.* **16**(2), 323–334 (2012) 486
487

16. R. Goldenthal, D. Harmon, R. Fattal, M. Bercovier, E. Grinspun, Efficient simulation of inextensible cloth, in *ACM Transactions on Graphics, SIGGRAPH'07* (2007) 488
489

17. M.A. Gondal, Exponential Rosenbrock integrators for option pricing. *J. Comput. Appl. Math.* **234**(4), 1153–1160 (2010) 490
491

18. E. Hairer, G. Wanner, *Solving Ordinary Differential Equations II: Stiff and Differential-Algebraic Problems* (Springer, New York, 1996) 492
493

19. M. Hauth, O. Etzmüller, A high performance solver for the animation of deformable objects using advanced numerical methods. *Comput. Graph. Forum* **20**, 319–328 (2001) 494
495

20. N.J. Higham, *Functions of Matrices: Theory and Computation* (SIAM, Philadelphia, 2008) 496

21. M. Hochbruck, C. Lubich, On Krylov subspace approximations to the matrix exponential operator. *SIAM J. Numer. Anal.* **34**, 1911–1925 (1997) 497
498

22. M. Hochbruck, A. Ostermann, Explicit exponential Runge–Kutta methods for semilinear parabolic problems. *SIAM J. Numer. Anal.* **43**, 1069–1090 (2005) 499
500

23. M. Hochbruck, A. Ostermann, Explicit integrators of Rosenbrock-type. *Oberwolfach Rep.* **3**, 501
1107–1110 (2006) 502

24. M. Hochbruck, A. Ostermann, Exponential integrators. *Acta Numer.* **19**, 209–286 (2010) 503

25. M. Hochbruck, C. Lubich, H. Selhofer, Exponential integrators for large systems of differential equations. *SIAM J. Sci. Comput.* **19**, 1552–1574 (1998) 504
505

26. M. Hochbruck, A. Ostermann, J. Schweitzer, Exponential Rosenbrock-type methods. *SIAM J. Numer. Anal.* **47**, 786–803 (2009) 506
507

27. S. Krogstad, Generalized integrating factor methods for stiff PDEs. *J. Comput. Phys.* **203**(1), 508
72–88 (2005) 509

28. M.W. Kutta, Beitrag zur näherungsweisen Integration totaler Differentialgleichungen. *Z. Math. Phys.* **46**, 435–453 (1901) 510
511

29. V.T. Luan, Fourth-order two-stage explicit exponential integrators for time-dependent PDEs. *Appl. Numer. Math.* **112**, 91–103 (2017) 512
513

30. V.T. Luan, A. Ostermann, Exponential B-series: the stiff case. *SIAM J. Numer. Anal.* **51**, 3431–3445 (2013) 514
515

31. V.T. Luan, A. Ostermann, Explicit exponential Runge–Kutta methods of high order for parabolic problems. *J. Comput. Appl. Math.* **256**, 168–179 (2014) 516
517

32. V.T. Luan, A. Ostermann, Exponential Rosenbrock methods of order five—construction, analysis and numerical comparisons. *J. Comput. Appl. Math.* **255**, 417–431 (2014) 518
519

33. V.T. Luan, A. Ostermann, Stiff order conditions for exponential Runge–Kutta methods of order five, in *Modeling, Simulation and Optimization of Complex Processes - HPSC 2012*, H.B. et al. (ed.) (Springer, Berlin, 2014), pp. 133–143 520
521
522

34. V.T. Luan, A. Ostermann, Parallel exponential Rosenbrock methods. *Comput. Math. Appl.* **71**, 523
1137–1150 (2016) 524

35. V.T. Luan, J.A. Pudykiewicz, D.R. Reynolds, Further development of the efficient and accurate time integration schemes for meteorological models. *J. Comput. Sci.* **376**, 817–837 (2018) 525
526

36. D.L. Michels, M. Desbrun, A semi-analytical approach to molecular dynamics. *J. Comput. Phys.* **303**, 336–354 (2015) 527
528

37. D.L. Michels, J.P.T. Mueller, Discrete computational mechanics for stiff phenomena, in *SIGGRAPH ASIA 2016 Courses* (2016), pp. 13:1–13:9 529
530

38. D.L. Michels, G.A. Sobottka, A.G. Weber, Exponential integrators for stiff elastodynamic problems. *ACM Trans. Graph.* **33**(1), 7:1–7:20 (2014) 531
532

39. D.L. Michels, J.P.T. Mueller, G.A. Sobottka, A physically based approach to the accurate simulation of stiff fibers and stiff fiber meshes. *Comput. Graph.* **53B**, 136–146 (2015) 533
534

40. D.L. Michels, V.T. Luan, M. Tokman, A stiffly accurate integrator for elastodynamic problems. *ACM Trans. Graph.* **36**(4), 116 (2017) 535
536

41. J. Niesen, W.M. Wright, Algorithm 919: a Krylov subspace algorithm for evaluating the φ -functions appearing in exponential integrators. *ACM Trans. Math. Softw.* **38**, 3 (2012) 537
538

42. D.A. Pope, An exponential method of numerical integration of ordinary differential equations. *Commun. ACM* **6**, 491–493 (1963) 539
540

43. C.D. Runge, Über die numerische Auflösung von Differentialgleichungen. *Math. Ann.* **46**, 167–178 (1895) 541
542

44. A. Stern, M. Desbrun, Discrete geometric mechanics for variational time integrators, in *SIGGRAPH 2006 Courses* (2006), pp. 75–80 543
544

45. A. Stern, E. Grinspun, Implicit-explicit variational integration of highly oscillatory problems. *Multiscale Model. Simul.* **7**, 1779–1794 (2009) 545
546

46. A. Tambue, I. Berre, J.M. Nordbotten, Efficient simulation of geothermal processes in heterogeneous porous media based on the exponential Rosenbrock–Euler and Rosenbrock-type methods. *Adv. Water Resour.* **53**, 250–262 (2013) 547
548
549

47. D. Terzopoulos, J. Platt, A. Barr, K. Fleischer, Elastically deformable models. *ACM Trans. Graph.* **21**, 205–214 (1987) 550
551

48. M. Tokman, J. Loffeld, P. Tranquilli, New adaptive exponential propagation iterative methods of Runge–Kutta type. *SIAM J. Sci. Comput.* **34**, A2650–A2669 (2012) 552
553

49. H. Zhuang, I. Kang, X. Wang, J.H. Lin, C.K. Cheng, Dynamic analysis of power delivery network with nonlinear components using matrix exponential method, in *2015 IEEE Symposium on Electromagnetic Compatibility and Signal Integrity* (IEEE, Piscataway, 2015), pp. 248–252 554
555
556

AUTHOR QUERIES

- AQ1.** Please check if the affiliations are presented correctly.
- AQ2.** Chapter title footnote has been moved to acknowledgement section. Please check and correct if necessary.
- AQ3.** Please provide complete details for Ref. [8].

Uncorrected Proof